J Geod
DOI 10.1007/s00190-010-0371-9

ORIGINAL ARTICLE

Single receiver phase ambiguity resolution with GPS data

Willy Bertiger · Shailen D. Desai · Bruce Haines · Nate Harvey · Angelyn W. Moore · Susan Owen · Jan P. Weiss

Received: 10 December 2009 / Accepted: 11 February 2010

Abstract Global positioning system (GPS) data processing algorithms typically improve positioning solution accuracy by fixing double-differenced phase bias ambiguities to integer values. These "double-difference ambiguity resolution" methods usually invoke linear combinations of GPS carrier phase bias estimates from pairs of transmitters and pairs of receivers, and traditionally require simultaneous measurements from at least two receivers. However, many GPS users point position a single local receiver, based on publicly available solutions for GPS orbits and clocks. These users cannot form double differences. We present an ambiguity resolution algorithm that improves solution accuracy for single receiver point-positioning users. The algorithm processes dual-frequency GPS data from a single receiver together with wide-lane and phase bias estimates from the global network of GPS receivers that were used to generate the orbit and clock solutions for the GPS satellites. We constrain (rather than fix) linear combinations of local phase biases to improve compatibility with global phase bias estimates. For this precise point positioning, no other receiver data are required. When tested, our algorithm significantly improved repeatability of daily estimates of ground receiver positions, most notably in the east component by approximately 30% with respect to the nominal case wherein the carrier biases are estimated as real values. In this "static" test for terrestrial receiver positions, we achieved daily repeatability of 1.9, 2.1 and 6.0 mm in the east, north and vertical (ENV) components, respectively. For kinematic solutions, ENV repeatability is 7.7, 8.4, and 11.7 mm, respectively, representing improvements of 22, 8, and 14% with respect to the nominal. Results from precise orbit determination of the twin GRACE satellites demonstrated that the inter-satellite baseline accuracy improved by a factor of three, from 6 to 2 mm up to a long-term bias. Jason-2/Ocean Surface Topography Mission precise orbit determination tests results implied radial orbit accuracy significantly below the 10 mm level. Stability of time transfer, in low-Earth orbit, improved from 40 to 7 ps. We produced these results by applying this algorithm within the Jet Propulsion Laboratory's (JPL's) GIPSY/OASIS software package and using JPL's orbit and clock products for the GPS constellation. These products now include a record of the wide-lane and phase bias estimates from the underlying global network of GPS stations. This implies that all GIPSY–OASIS positioning users can now benefit from this capability to perform single-receiver ambiguity resolution.

Keywords Ambiguity fixing · GPS · POD · Precise point positioning · WLPBLIST

W. Bertiger (✉) · S. D. Desai · B. Haines · N. Harvey · A. W. Moore · S. Owen · J. P. Weiss
Jet Propulsion Laboratory, California Institute of Technology, Pasadena, CA, USA
e-mail: willy.bertiger@jpl.nasa.gov

1 Introduction

Since the 1980s, global positioning system (GPS) data processing algorithms, which estimate positions and other parameters, have frequently "resolved ambiguities"—fixed linear combinations of phase bias estimates—to improve solution accuracy (Blewitt 1989). Until recently, ambiguity resolution algorithms explicitly differenced phase bias estimates, or phase bias data, from a pair of receivers and a pair of transmitters, in order to cancel receiver and transmitter hardware delays. Dual-frequency ambiguity resolution algorithms typically require two steps: resolution of the wide-lane, followed by resolution of the narrow-lane (Melbourne 1985; Wubbena 1985).

Published online: 21 March 2010

During the past few years, several authors have suggested hardware delay calibration, allowing ambiguity resolution at a single dual-frequency receiver (Laurichesse et al. 2008). Laurichesse et al. (2008) calibrated GPS transmitter wide-lane delays to allow single-receiver wide-lane resolution, and produced a special "integer" GPS clock solution to allow single-receiver narrow-lane resolution. Satellite Laser Ranging (SLR) data, compared to pre- and post-resolution results, strongly indicated improved Jason-1 orbit solutions. A single GRACEA/GRACEB test day registered 2- mm relative accuracy, accepting as truth the micron-level accurate GRACE K-Band ranging system, up to an overall bias in each connected K-band arc on each day (Dunn et al. 2003).

We present a different approach to single-receiver ambiguity resolution, implemented in a complete operational system that computes bias-resolved solutions for low earth orbiting (LEO) or ground receivers, running the Jet Propulsion Laboratory's (JPL's) GIPSY–OASIS software. Our system requires orbit, clock, wide-lane and phase bias information, computed by GIPSY–OASIS operational processes. Orbit, clock, wide-lane and phase bias information from the JPL International GNSS Service (IGS) (Dow et al. 2009) Analysis Center's contribution to the IGS products, http://igscb.jpl.nasa.gov/components/prods.html, are available via anonymous ftp at ftp://sideshow.jpl.nasa.gov/pub/JPL_GPS_Products.

Like all IGS analysis centers, JPL solves for GPS orbits and clocks by processing data from a globally distributed set of static ground receivers. In addition, we save wide-lane (WL) and dual-frequency phase bias (PB) estimate information for each phase-connected GPS data arc processed during our global computation, in a small (<200 kB) wide-lane phase bias information, or WLPBLIST, file. A WLPBLIST contains a line for each continuously tracked phase arc in our global solution. Each line records GPS transmitting satellite name, GPS ground receiver name, phase arc start time, phase arc stop time, estimated wide-lane value, and the estimated dual-frequency phase bias for this arc.

To resolve ambiguities while point positioning a single local receiver, we form double difference combinations of local phase bias estimates, from our current run, and global phase bias estimates, drawn from the WLPBLIST file. The values of the phase bias in the WLPBLIST file are relative to the assumed antenna offsets. For the time period tested here, this has been the IGS recommended standard. The values have changed only for the addition of new GPS satellites and receiver antenna types. The exact antenna calibration used is recorded and made published with the WLPBLIST. We then add constraint equations in our Kalman filter/smoother to nudge double differences towards integer values. The next section of this note presents our algorithm in more detail.

JPL began operational production of the WLPBLIST files in 2009, and they are being generated as part of our efforts to reprocess historical GPS data from 1994 to 2009. The WLPBLIST files are now included in JPL's delivery of GPS orbit and clock products for GIPSY/OASIS users. A GIPSY/OASIS user, using version 5.1 and higher, can therefore produce an ambiguity-resolved point-positioning solution for a single receiver with a single command (gd2p.pl) that requires a few command line arguments.

2 Algorithm description

We designed a variant of the standard (ionosphere-free wide-lane) double difference ambiguity resolution algorithm described by Blewitt (1989) to resolve ambiguities at a single receiver based on a global network solution.

Roughly described, the algorithm in Blewitt (1989) does the following.

1) For every receiver A and every transmitter I, define

$$\begin{aligned} n_1(I,A) &\equiv \text{integer ambiguity in } L_1 \text{ carrier phase cycle count} \\ n_2(I,A) &\equiv \text{integer ambiguity in } L_2 \text{ carrier phase cycle count} \\ n_W(I,A) &\equiv n_1(I,A) - n_2(I,A) \end{aligned}$$

2) At every epoch, for every pair of receivers {A, B} and every pair of transmitters {I, II} in common view, double difference ionosphere-free wide-lanes (WL) (Melbourne 1985; Wubbena 1985) to resolve $\Delta\Delta n_W$.

$$\mathrm{WL} = \left(\frac{f_1 \cdot L_1 - f_2 \cdot L_2}{f_1 - f_2}\right) - \left(\frac{f_1 \cdot P_1 + f_2 \cdot P_2}{f_1 + f_2}\right)$$

$$\begin{aligned} \Delta\Delta n_W(\{I,II\},\{A,B\}) &\equiv n_W(I,A) - n_W(II,A) \\ &\quad - n_W(I,B) + n_W(II,B) \\ &\approx \mathrm{WL}(I,A) - WL(II,A) \\ &\quad - \mathrm{WL}(I,B) + WL(II,B) \end{aligned}$$

3) Having identified $\Delta\Delta n_W$, double difference dual frequency phase bias (PB) estimates from the Kalman filter/smoother, form the narrow-lane double-difference combination, and resolve $\Delta\Delta n_1$.

$$\Delta\Delta n_1(\{I,II\},\{A,B\}) = \frac{\Delta\Delta PB(\{I,II\},\{A,B\}) - \lambda_D \cdot \Delta\Delta n_W(\{I,II\},\{A,B\})}{\lambda_N}$$

$$\lambda_D \approx 1.98 \cdot \lambda_1$$

$$\lambda_N \approx 10.7\text{cm}$$

4) Having identified $\Delta\Delta n_W$ and $\Delta\Delta n_1$, apply a hard constraint to the phase bias double difference. Since we constrain double differences tightly, we only need to resolve a maximal linearly independent set of ambiguities.

$$\begin{aligned}&\Delta\Delta \mathrm{PB}\left(\{I, II\}, \{A, B\}\right)\\&\quad \equiv \mathrm{PB}\left(I, A\right) - \mathrm{PB}\left(II, A\right) - \mathrm{PB}\left(I, B\right) + \mathrm{PB}\left(II, B\right)\\&\quad = \lambda_D \cdot \Delta\Delta n_W + \lambda_N \cdot \Delta\Delta n_1\end{aligned}$$

Our single receiver ambiguity resolution algorithm differs from the (ionosphere-free wide-lane) algorithm described in Blewitt (1989) in the following ways.

1) Process data from a global network of GPS stations (with network ambiguity resolution) to position GPS stations and satellites and solve for their respective clocks. Save information about phase biases and wide-lanes from arcs in the global solution to a WLPBLIST file that is subsequently made available to point-positioning users.
2) Point position the single receiver of interest based on the global network solution of GPS orbits and clocks.
3) Processing information from our single-receiver point positioning run, and global arc information from the WLPBLIST, form a list of possible double differences involving the local receiver being point-positioned (L), a station from the global network solution (G), and a pair of transmitters {I, II} in common view. No observational data is needed for this list from the global stations or transmitters. Only the time intervals from the WLPBLIST file are required and the local receiver information.
4) Double difference wide-lanes to resolve $\Delta\Delta n_W$ using wide-lane estimates for station G from the WLPBLIST file,
5) Having identified $\Delta\Delta n_W$, read phase bias estimates for station G from the WLPBLIST file and double difference phase bias estimates to resolve $\Delta\Delta n_1$.
6) Having identified $\Delta\Delta n_W$ and $\Delta\Delta n_1$, apply a soft constraint to the phase bias double difference. We apply a soft constraint rather than a hard constraint to allow for inaccuracies in the global solution, and because the probability of mis-resolution is typically fairly high. Since we constrain ambiguities loosely, we resolve every ambiguity we can, rather than restrict ourselves to a linearly independent set of ambiguities.
7) If necessary, iterate steps 3)–6) to converge towards a better solution.

Since we apply single receiver ambiguity resolution in a variety of situations, ranging from static GPS ground receivers to low-Earth orbiting (LEO) satellites, our algorithm and software allows the user to specify a number of variables and options, some of which are worth mentioning here.

1) Double-differencing wide-lanes cancels receiver and transmitter hardware wide-lane biases. If these hardware biases remain stable from epoch to epoch over the length of an arc, we can use every available point in all four arcs of the double difference to estimate $\Delta\Delta n_W$. On the other hand, if hardware delays vary from epoch to epoch, biases only cancel if we double-difference wide-lane observations at a common epoch. GPS transmitter wide-lane biases are fairly stable. Wide-lane biases at most (but not all) IGS stations are also stable, but some other networks contain a high proportion of stations with unstable wide-lane receiver biases. Since LEO receivers process much shorter arcs, wide-lane biases drift less over the length of an arc, and the relative advantage of using every available point is more significant. Lacking information to the contrary, we typically assume stable wide-lane biases for LEO receivers, and unstable biases for ground stations.
2) At well-behaved receiver pairs, mis-resolved wide-lanes are usually off by +/− 1 cycle, which results in a narrow-lane bias of +/− 0.53 cycles (modulo an integer) conveniently far away from any integer. Usually, we take advantage of this behavior when computing ambiguity resolution confidence. Unfortunately, for the Jason-2 GPS receiver, half-cycle issues in phase data complicate resolution (Bertiger et al. 2010), so we apply a cruder confidence calculation that does not assume integer-based behavior.
3) With shorter arcs, both the wide-lane and the narrow-lane are harder to resolve at a LEO receiver than at a static ground station, so we accept a lower confidence level. To compensate for lower confidence, we apply looser constraints to resolved ambiguities. These looser constraints do not affect the final result as effectively, so we iterate ambiguity resolution when positioning a LEO, usually 10 times (a number chosen by trial and error). We typically do not iterate when positioning a static ground station.

3 Low earth orbiter results

Since the TOPEX/Poseidon satellite launched in 1992, a number of LEO satellites whose missions require precisely determined orbits have carried GPS receivers (Bertiger et al. 1994). For this investigation, we studied GPS data processing results from two LEO missions:

1) Jason-2/Ocean Surface Topography Mission (OSTM) satellite (Neeck and Vaze 2008), is a follow-on to TOPEX/Poseidon, in a 1,300 km altitude orbit. It carries a radar altimeter to measure sea surface height. Spacecraft radial position estimates directly affect sea surface

height estimates. Data are processed at JPL by an automated operational system that has used single receiver ambiguity resolution since June 2009.

2) Gravity Recovery and Climate Experiment (GRACE) mission, twin satellites (GRACEA and GRACEB) in a common orbit at 500 km altitude, separated by 200 km. A K-band biased ranging system between the two GRACE satellites measures separation, up to a bias, with micron-level accuracy (Dunn et al. 2003). Twin spacecraft serve as test masses for recovery of Earth's mass distribution (Tapley et al. 2004). K-band ranging requires time synchronization between GRACEA and GRACEB with better than 150 ps accuracy to meet mission requirements. The synchronization is accomplished by processing GPS data for GRACEA/B orbital positions and clocks. Data are processed daily at JPL by an automated operational system which has used single receiver ambiguity resolution since 1 May 2009. Necessary but not sufficient tests of the 150 ps requirement are presented below.

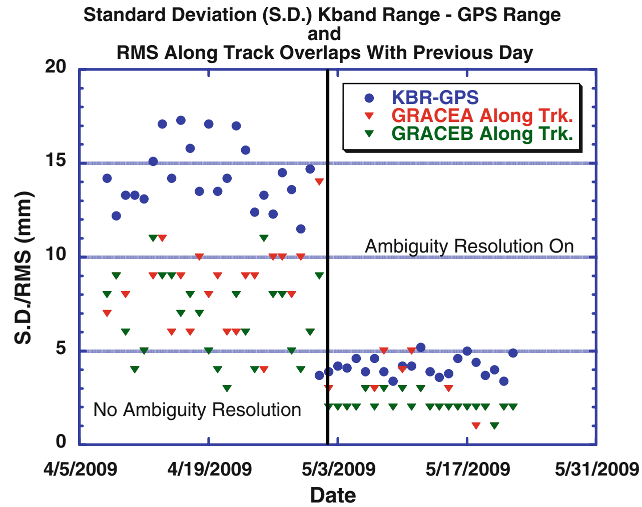

Fig. 1 Kband Range–GPS Range and along track overlaps. KBR–GPS improved dramatically on 1 May, when ambiguity resolution began, overlap improvement for GRACEA and GRACEB lags a day since they are computed by comparison with the previous day

3.1 GRACE results

The operational processing of the GRACE data to synchronize time between the GRACE spacecraft and form the micron-level dual one-way K-band measurement was changed on 1 May 2009 to use the bias resolution method for a single receiver. Double-differenced biases between the two GRACE satellites are not formed, and POD for each of the twins is performed independently. In the operational system, the GPS phase data are decimated to 5-min points and the pseudorange data are carrier smoothed to 5-min points. We routinely monitor several system performance statistics.

1) Standard deviation of (K-Band biased range—GPS-based positioning range). The GRACEA/B range is computed from independent GPS data processing orbital solutions for each satellite and compared to the K-band measurements. The standard deviation of the difference is computed on each continuous K-band arc on each day (since K-band rarely loses lock, typically only one arc per day, very seldom more than three). By the nature of K-band tracking, each continuous K-band arc has one undetermined bias, which we remove by least-squares estimation. Even after removal of a bias, GRACEA/B baseline length varies complexly with time, exhibiting features ranging from micron-level to meter-level.
2) RMS orbit overlaps. On each day, we compute GRACE orbit solutions by processing 30 h of GPS data centered on that day, so each day's solution overlaps with the previous day's solution for 6 h. The RMS of the difference is computed over the center 5 h of the 6-h overlap, and separated into radial, cross-track, and along-track components. This 5 h time span starts at 21:30 on the first day and ends at 02:30 on the second day.
3) (GRACEA–GRACEB) relative clock overlaps. The (GRACEA–GRACEB) relative clock solution is computed on each day and the mean and standard deviation of relative clock solution differences from day-to-day are computed using the center 5 h of the 6-h overlap.

Figures 1 and 2 display results for these three metrics from GRACE operational processing before (7 April 2009 to 30 April 2009) and after (1–22 May 2009) we added single receiver ambiguity resolution to our automatic process. The average (K-band biased range - GPS range) daily standard deviation improved from 14.3 to 4.1 mm, a factor of more than 3. Along-track mean RMS overlaps for GRACEA improved from 8.0 to 2.5 mm, and for GRACEB from 6.8 to 2.1 mm. Relative clock solution average standard deviation improved from 41.0 to 7.2 ps, while the mean relative clock differences did not improve by a comparable factor, probably because pseudorange data dominates determination of mean relative clocks. Improved P-code antenna calibrations for GPS transmitters might improve the mean relative clock consistency. Our automated process currently uses IGS-recommended antenna calibrations, which do not distinguish between code and phase data types.

The GPS receivers on-board GRACE sample pseudorange at 10-s intervals and phase every second. In the past, our system estimating GPS orbits and clocks routinely produced GPS clock values at 5-min intervals, but did not routinely produce them at higher rates (Jefferson et al. 1999). Our current system routinely produces 30-s GPS clock solutions, which enables improved processing of higher rate GRACE

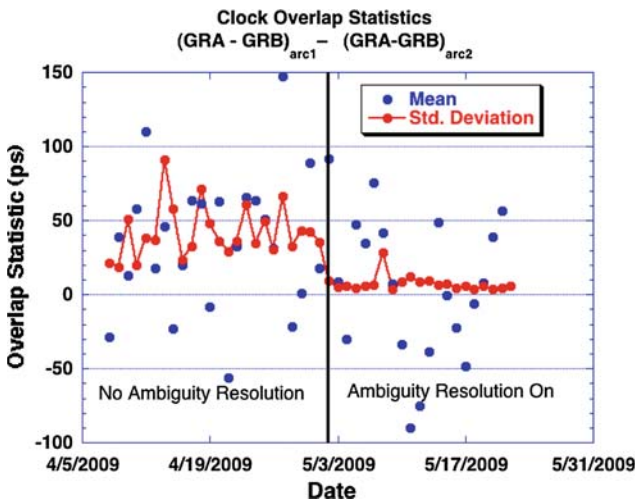

Fig. 2 Operational clock synchronization statistics before and after ambiguity resolution

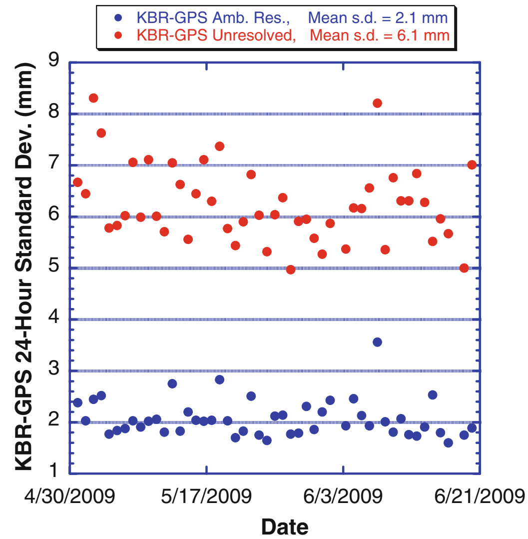

Fig. 3 Benefits of single receiver ambiguity resolution for GRACE baseline determination using 30-s data. Accuracy measured by the K-band instrument (KBR)

data. While our results with 5-min data meet mission requirements, processing 30-s data gives better results (Jäggi et al. 2009). Jäggi's team examined the effects of antenna calibration techniques on GRACE precision orbit determination (POD). The best solution over the best 60-day time period (in 2007) cited in their paper gave a KBR-GPS range mean daily standard deviation (SD) of 5.9 mm, processing 30-s data. When they double-differenced data between GRACEA and GRACEB, and resolved ambiguities, mean SD for all of 2007 (excluding a few days) improved to 0.81 mm, improving on a previous result (Kroes 2006) without antenna calibration.

One would expect a further improvement in baseline determination when fixing double differences directly between GRACEA and GRACEB, from direct cancellation of common mode errors (e.g., Kroes 2006). In this note, however, we focus only on single receiver ambiguity resolution, applicable to single-satellite LEO missions.

Table 1 Stochastic acceleration parameters; operational and re-tuned strategy

Parameter	Process noise (nm/s^2)	Update (s)	Time correlation (s)
Operations			
Constant along track	300	300	1, 800
Constant radial	50	300	1,800
Constant cross-track	100	300	1,800
Re-tuned			
Constant along track	30	300	7,200
Constant radial	5	300	7,200
Constant cross track	10	300	7,200
1/rev along track	5	6,750	21,600
1/rev cross track	5	6,750	21,600

We re-processed GRACE data from 1 May 2009 to 20 June 2009, using 30-s rather than 5-min samples. Simply processing the data at the 30-s rate did not significantly improve the key KBR-GPS metric, so we also adjusted our empirical stochastic acceleration parameters. Table 1 contrasts the nominal parameterization for processing the 5-min. data in the operational process with the tuned solution strategy adopted for the 30-s data. The most significant difference is the addition of an empirical once-per-revolution acceleration. With a 5-min data rate bias resolved orbits improved the KBR-GPS range standard deviation from 4.1 to 2.9 mm when the operational parameterization in Table 1 was replaced with the re-tuned parameters for the test period. Processing 30-s data with the tuned parameter set yielded KBR-GPS agreement at the 6.1 and 2.1 mm level (mean of the standard deviation) before and after single receiver ambiguity resolution (Fig. 3). Figure 4 shows GRACEA orbit overlaps for 30-s data and re-tuned parameters with Table 2 summarizing the daily statistics.

3.2 Jason-2/Ocean Surface Topography Mission

Launched 20 June 2008, Jason-2/Ocean Surface Topography Mission (OSTM) carries a radar altimeter that measures satellite-ocean separation with roughly 3-cm accuracy at 1 Hz sampling (Neeck and Vaze 2008). Jason-2 also carries three measurement systems for orbit determination from GPS, Satellite Laser Ranging (SLR), and Doppler Orbitography and Radiopositioning Integrated by Satellite (DORIS) data. The French space agency, Centre National d'Études

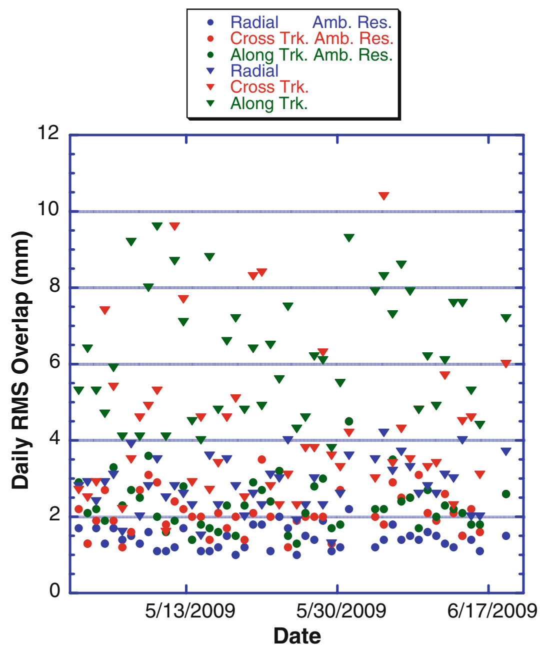

Fig. 4 GRACEA 5-h RMS overlaps, 30-s data rate, re-tuned parameters, with and without ambiguity resolution. *Closed circles* indicate ambiguity resolved RMS overlaps

Spatiales (CNES), produces official orbits for geophysical data records (GDR) based on GPS, SLR, and DORIS data (Cerri et al. 2010).

Jason-2/OSTM orbits at a substantially higher altitude than do the GRACE satellites, 1,300 km rather than 500 km, which affects positioning in two ways; one helpful, one harmful.

1) Less atmosphere, so lower drag, at 1,300 km, reduces errors in our force model, allowing a more dynamic model, less affected by bad or missing data.
2) The radiation environment is significantly harsher at 1,300 km, forcing frequent GPS receiver resets, which concentrate near the South Atlantic Anomaly.

Jason-2/OSTM model details may be found in Bertiger et al. (2010). We applied three metrics to assess the effect of single receiver ambiguity resolution on Jason-2 orbit estimate precision, with results summarized in the next two tables and a figure.

1) *RMS orbit overlaps* from July 2008 to June 2009 (Table 3): On each day, we solve for Jason-2 orbits processing 30 h of data centered on noon, so each day's solution overlaps with the previous day's solution for 6 h. The RMS difference over the center 4 h of the 6-h overlap is computed and separated into radial, cross-track, and along-track components, before and after single receiver ambiguity resolution. The radial component, key for Jason-2/OSTM, improved by a factor of 1.7.
2) *Scatter of SLR residuals* from July 2008 to May 2009 (Table 4): We produced orbit solutions by processing only GPS data, so SLR data provide an independent validation of our pre- and post-ambiguity resolution orbits. Since Jason-2 requirements address only radial accuracy, we restricted our consideration to SLR data above 60° elevation as viewed from the ground. To reduce SLR measurement error, we focused on four of the highest quality SLR ground stations: Monument, Yaragadee, Graz and McDonald. Ambiguity resolution improved scatter substantially at all four stations. Our ambiguity resolved results compare favorably with CNES's official results (GDR-C) (Cerri et al. 2010), which did fit to the SLR data. Typical scatter, pre and post-ambiguity resolution, lies below a centimeter, suggesting sub-centimeter radial accuracy, up to an overall bias.
3) *Differences of sea-surface height (SSH) estimates at crossover locations* (Fig. 5): The data from the radar altimeter are used in neither the CNES-determined orbits nor the JPL GPS-determined orbits discussed here. At the locations where the ground track paths from ascending and descending passes cross each other on the ocean surface, we can use the difference in the radar altimeter's measurement of the SSH to infer relative radial orbit error. At the crossover points, the radial orbit error is fully expressed in the SSH error. In addition to the orbit error, however, there are measurement errors in the radar and true changes in SSH due to different sampling times at the crossover point. In order to minimize these other error sources, we examine only those crossover points for which the ascending and descending passes are separated by fewer than three days with moderately calm oceans (significant wave heights of 1–4 m and surface wind speeds of 4–10 m/s) and with the absolute value of atmospheric pressure loading correction less than 15 cm. We refer to this selection process as super-editing. Since Jason-2/OSTM repeats its ground track on the Earth every 10 days, we computed the variance of the sea height crossover difference over each of these 10-day cycles. Figure 5, shows the reduction in crossover variance between the orbits determined with and without ambiguity resolution. A positive value indicates that ambiguity resolution reduced crossover variance. The variance is reduced on all 26 10-day cycles with an average reduction of 45 mm^2.

4 Static ground receiver and baseline results

To test the new single receiver method on static ground receiver positioning, we examined station coordinate repeatability before and after ambiguity resolution. Table 5 shows

Table 2 Mean RMS overlaps with and without ambiguity resolution, 1 May 2009 through 20 June 2009, 30-s data, re-tuned parameters

	Radial (mm)	Radial Amb. Res. (mm)	Cross Trk. (mm)	Cross Trk. Amb. Res. (mm)	Along Trk. (mm)	Along Trk. Amb. Res. (mm)
GRACEA	2.8	1.4	4.4	2.2	6.3	2.3
GRACEB	2.9	1.4	4.2	2.1	6.3	2.3

Table 3 Average RMS overlaps from consecutive 30-h processing arcs, 11 July 2008 through 5 June 2009

	Radial (mm)	Radial Amb. Res. (mm)	Cross Trk. (mm)	Cross Trk. Amb. Res. (mm)	Along Trk. (mm) (mm)	Along Trk. Amb. Res. (mm)
Jason-2/OSTM	3.1	1.8	3.6	3.0	7.6	4.6

Table 4 For each SLR tracking pass the mean of the one-way SLR range residual is computed. The standard deviation (sigma) and mean of these biases are computed for three different Jason-2/OSTM orbits 12 July 2008 through 31 May 2009

	CNES, GDR-C sigma/mean (mm)	JPL reduced dynamic sigma/mean (mm)	JPL ambiguity resolved sigma/mean (mm)	# Arcs
Monument	8.6/10.2	8.1/10.1	6.4/10.8	20
Yaragadee	6.5/2.1	7.9/7.8	6.2/9.0	190
Graz	6.5/ − 6.8	10.3/ − 9.6	8.0/ − 8.9	75
McDonald	8.8/ − 6.8	9.9/9.6	8.3/10.5	19
All (weighted)	6.8/1.1	8.7/3.8	6.8/4.8	304

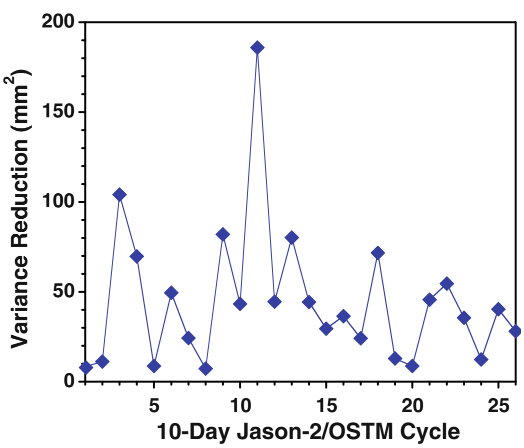

Fig. 5 Difference in sea height variance at super-edited cross-over points (variance without ambiguity resolution)–(variance with ambiguity resolution), mean variance reduction is 45 mm^2

key parameter assumptions for static positioning. The static point positioning procedure is similar to the one in Zumberge et al. (1997), but with updated models and more highly automated software. Troposphere and clock parameters are updated every 5 min and the GPS data are sampled every 5 min. We processed 6 months (1 June 2008 to 30 November 2008) of data from 209 stations in 24-h intervals. We ignore stations that have do not have quality data for at least 80% of the days. Figure 6 shows a map of the locations of the stations considered in this study. Table 6 summarizes the scatter about the IGS defined coordinates for the 106 stations that define the IGS05 frame. Results for each component (east, north, vertical) for two tropospheric mapping functions (Niell/VMF1) both with and without bias resolution are given. Bias resolution makes a significant improvement in the east component in both cases. There are only modest improvements in the other components due to bias resolution. The newer VMF1 troposphere model makes a significant improvement in the vertical component as seen by others (Boehm et al. 2006).

Bias fixing has traditionally been used on baselines where the data may be explicitly double differenced to remove hardware delays. This method has long been implemented in the GIPSY–OASIS software package and is part of many other GPS software systems as well. Here we compare baseline results using our new single station bias resolution method and the method implemented in GIPSY–OASIS based on Blewitt (1989). The software wrapping Blewitt's algorithm in GIPSY–OASIS is referred to as the "Network Processor" (Liu et al. 2009; Owen et al. 2006). We processed 301 baselines from 1 June 2008 to 30 November 2008, using IGS station data. Only baselines between 10 and 10,000 km are considered. Figure 7 shows the daily scatter about the mean as a function of baseline length (log scale) for each of the 301 baselines considered and a linear fit to the scatter. We see that the daily scatter of the single station bias resolution method is approximately equivalent to that of the traditional double

Table 5 Parameters estimated and key models applied in 24-h static positioning tests

Parameter	Relevant model	Solution properties
Station coordinates	IERS03 Earth models (McCarthy and Petit 2004)	Constant over 24 h
Zenith troposphere delay	Niell (Niell 2006) or VMF1 mapping functions (Boehm et al. 2006)	Random walk 50 µm/sqrt (h)
Gradient troposphere delay	Bar-Sever et al. (1998)	Random walk 5 µm/sqrt (h)
Station clock		White-noise unconstrained

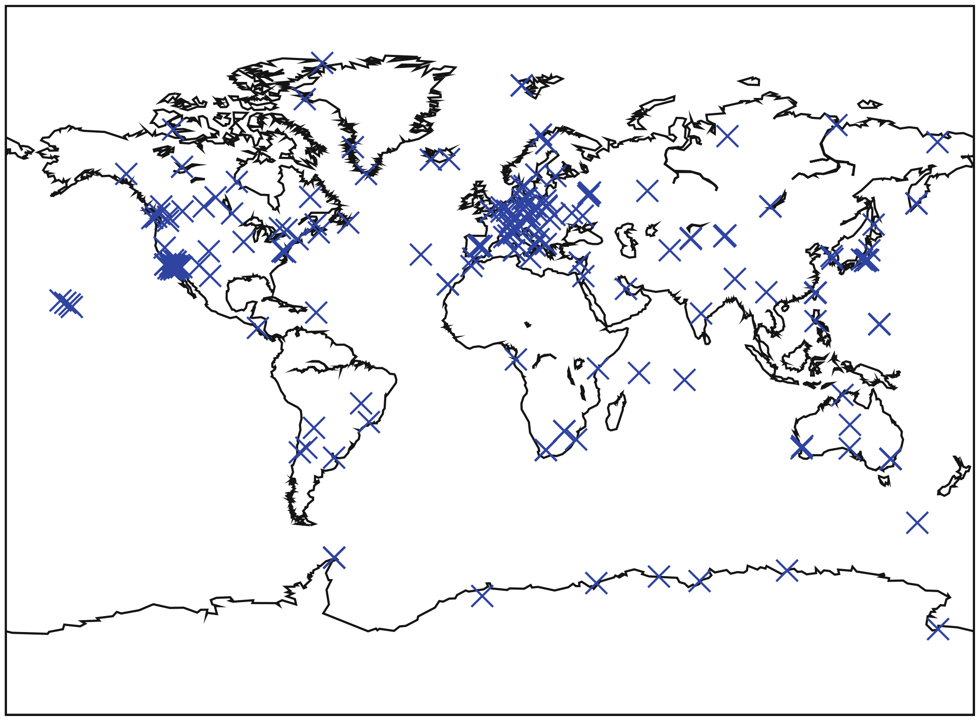

Fig. 6 Positions of the 209 stations considered in the baseline/station position calculations

Table 6 Standard deviation of the station east, north, and vertical components for 24-h static positioning from 1 June 2008 to 30 November 2008 using 106 IGS frame definition stations

	East (mm)	North (mm)	Vertical (mm)
Unresolved/Niell	2.9	2.1	7.0
Resolved/Niell	1.9	2.0	6.8
Unresolved/VMF1	2.9	2.1	6.0
Resolved/VMF1	1.9	2.1	6.0

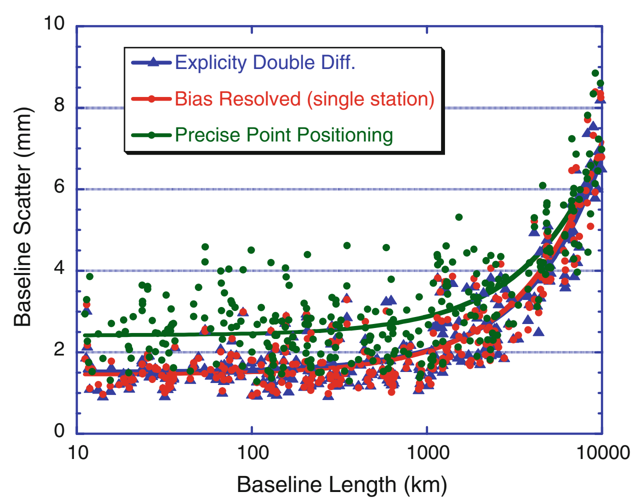

Fig. 7 The daily baseline scatter about the mean as a function of baseline is plotted for each of the 301 considered baselines along with a linear fit. The scatter in the single station ambiguity resolution (*red dot*) and traditional double difference ambiguity resolution (*blue triangle*) are shown along with the pre-resolution scatter (*green dot*), precise point positioning, phase biases adjusted as real numbers only, along with a linear fit in each case

difference method. The efficacy of both methods decay similarly as the length of the baseline increases. At the longest baselines, improvements with explicit double differences or bias resolution over precise point positioning are small (note that the number of samples at the longest baselines is also small).

Figure 8 shows another view of the baseline scatter for the same set of data as Fig. 7. The fractional improvement in baseline length repeatability as a function of baseline length is again indistinguishable.

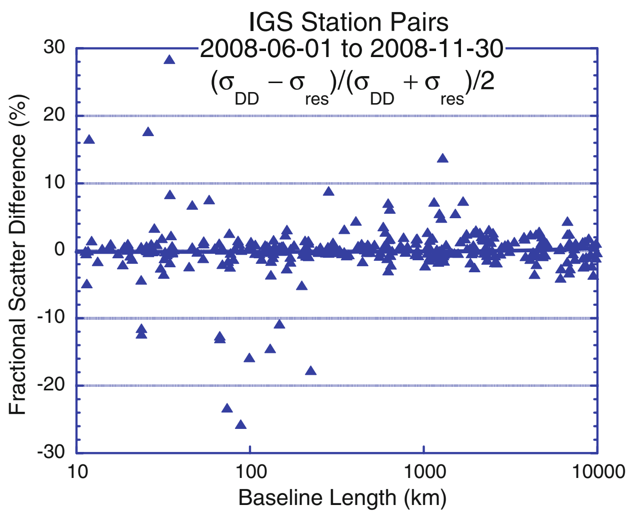

Fig. 8 Baseline scatter using double differenced (σ_{DD}) fixed phase ambiguities versus single receiver bias resolution (σ_{res})

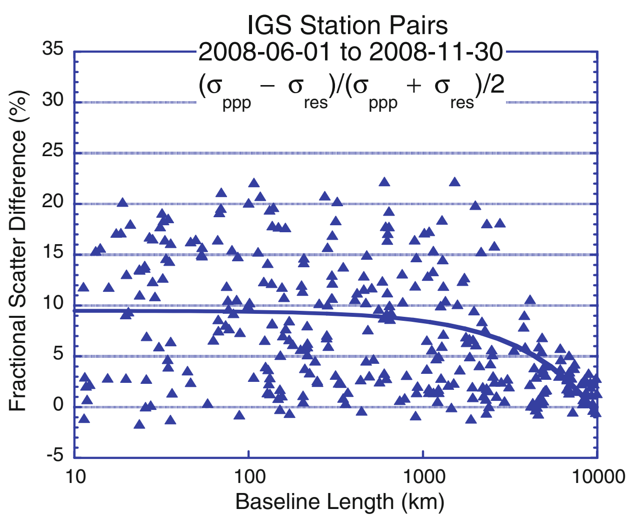

Fig. 9 Baseline determination over 24-h with precise point positioning (ppp) versus bias resolution (res), improvements in baseline length scatter

Finally, Fig. 9 compares the new bias resolution method to precise point positioning. For baselines under 1,000 km, bias resolution improves baseline repeatability by about 10%. The results for traditional double differencing, compared to precise point positioning without ambiguity resolution, would, of course, be the similar.

The IGS station distribution did not include many baselines in the range of 1–10 km. In order to study the methods in this regime we used 309 baselines from the Los Angeles California area in daily solutions during the month of June 2008. Figure 10 shows the scatter in baseline calculations. The average scatter for both explicit double differencing and bias resolution is 1.4 mm. The scatter in the unresolved precise point positioning is 2.2 mm; thus either method of bias

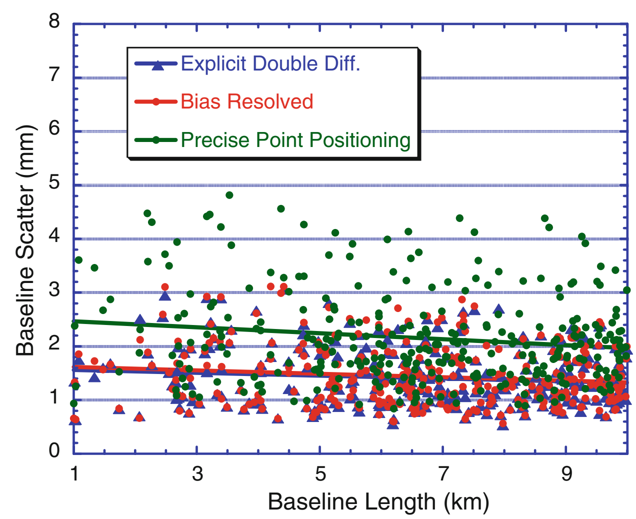

Fig. 10 The scatter of daily short baselines within the Los Angeles Basin for June 2008 is plotted as a function of baseline length. The average scatter for the single station ambiguity resolution and traditional ambiguity resolution is 1.4 mm, while the scatter of the unresolved baselines is 2.2 mm

adjustment improves short baselines by about 36% compared to precise point positioning. Although there is a slight slope to the linear fits shown in the plots, this may be due to the small number of samples at the shortest baseline lengths.

5 Kinematic ground receiver positioning

Kinematic point positioning of 15 static terrestrial GPS stations is performed with and without single receiver ambiguity resolution for the 6-month period from 12 April to 11 October 2009. The stations were selected from the IGS network and provide examples from different regions of the Earth, including island sites and sites on different continents. Kinematic solutions are generated for each day using 30 h of data centered at noon of each day, and with positions estimated at 5-min intervals. We first consider the scatter of the 5-min kinematic position solutions from the middle 24 h of the 30-h solution window with respect to the static point position solution for that day. Each of the 15 stations demonstrated a reduction in the median of its daily RMS of position differences in all three components. As shown in Table 7, the median of the daily RMS of these differences over all 2,559 station days improves in all three components, east, north and vertical, by 22, 9, and 14%, respectively. Days with incomplete or missing data are excluded from these statistics.

Second, there is a 6-h period in each day, where kinematic position solutions from neighboring days overlap. The scatter of the differences between the middle 4 h of these overlapping solutions is a measure of the impact of ambiguity resolution on the day-to-day consistency of kinematic point positioning

Table 7 Impact of ambiguity resolution on kinematic point positioning of 15 global GPS sites for 6-month period from 12 April to 11 October 2009

	Median of daily RMS of differences Between 5- min kinematic solutions and daily static solution		Median of daily RMS of differences Between overlapping kinematic solutions	
	No ambiguity resolution	With ambiguity resolution	No ambiguity resolution	With ambiguity resolution
East (mm)	9.9	7.7	7.1	3.0
North (mm)	9.2	8.4	4.3	2.7
Vertical (mm)	13.6	11.7	7.7	5.5

(last two columns of Table 7). Of the 15 stations considered, only the vertical component of the overlaps of one station, Tahiti, degraded by 10% when using ambiguity resolution, while all components of the other stations improved significantly. The median of the daily RMS of kinematic position overlap differences over all 2475 station days with overlaps improved by 58, 36, and 29% in the east, north and vertical components, respectively.

6 Summary

The new ambiguity resolution method integrating operational GPS orbit and clock products (ftp://sideshow.jpl.nasa.gov/pub/JPL_GPS_Products) and JPL's GPS receiver processing software (GIPSY-OASIS II, http://gipsy-oasis.jpl.nasa.gov/gipsy/software.html) can be used to process GPS data under a variety of circumstances. For static positioning of receivers on the surface of the Earth, the new method is competitive with traditional bias fixing methods used to determine baselines between two stations. The new method improves static precise point positioning of a single receiver, yielding repeatability in east, north, and vertical components of 1.9, 2.1, and 6.0 mm. Kinematic positioning with stochastic updates every 5 min improved with bias resolution in east, north, and vertical by about 22, 9, and 14% for a receiver on the Earth.

With single receiver ambiguity resolution, the baseline length between the two GRACE spacecraft may be determined to an accuracy of 2 mm up to a long-term constant. Relative time transfer has a precision of about 7 ps. Jason-2/OSTM was also used to test the bias resolution method. Radial orbit overlaps for Jason-2/OSTM improved from 3.1 to 1.8 mm and independent SLR ranging test show a scatter of 6.8 mm making a strong argument for radial orbit accuracy better than 1 cm. Independent radar altimeter cross-over analysis further confirm the effectiveness of bias resolution.

Acknowledgments The work described in this paper was performed at the Jet Propulsion Laboratory, California Institute of Technology, under contract with the National Aeronautics and Space Administration. The authors would like to thank our colleague Mark Miller for his extensive work in testing static positioning.

References

Bar-Sever YE, Kroger PM, Borjesson JA (1998) Estimating horizontal gradients of tropospheric path delay with a single GPS receiver. J Geophys Res 103:5019–5035

Bertiger W, Desai S, Dorsey A, Haines B, Harvey N, Kuang D, Sibthorpe A, Weiss J (2010) Sub-centimeter precision orbit determination with GPS for ocean altimetry. Mar Geod Spec Issue (submitted)

Bertiger WI, Bar-Sever YE, Christensen EJ, Davis ES, Guinn JR, Haines BJ, Ibanez-Meier RW, Jee JR, Lichten SM, Melbourne WG, Muellerschoen RJ, Munson TN, Vigue Y, Wu SC, Yunck TP, Schutz BE, Abusali PAM, Rim HJ, Watkins MM, Willis P (1994) GPS precise tracking Of TOPEX/Poseidon: results and implications. JGR Oceans TOPEX/Poseidon Spec Issue 99C12: 24,449–24,464

Blewitt G (1989) Carrier phase ambiguity resolution for the global positioning system applied to geodetic baselines up to 200 km. J Geophys Res 94B8:10187–10203

Boehm J, Werl B, Schuh H (2006) Troposphere mapping functions for GPS and very long baseline interferometry from European Centre for Medium-Range Weather Forecasts operational analysis data. J Geophys Res 111:B02406. doi:10.1029/2005JB003629

Cerri L, Mercier F, Berthias JP, Ries JC, Lemoine FG, Zelensky NP, Bertiger W, Haines B, Willis P, Ziebart M (2010) Precision orbit determination standards for the Jason series of altimeter missions. Mar Geod Spec Issue (submitted)

Dow JM, Neilan RE, Rizos C (2009) The International GNSS Service in a changing landscape of Global Navigation Satellite Systems. J Geod 83(7): 191–198. doi:10.1007/s00190-008-0300-3

Dunn C, Bertiger W, Bar-Sever Y, Bettadpur S, Desai S, Franklin G, Haines B, Kruizinga G, Kuang D, Meehan T, Nandi S, Nguyen D, Rogstad T, Romans L, Thomas BJ, Tien J, Watkins M, Wu S (2003) Instrument of grace, GPS augments gravity measurements. GPS World 14(2):16–28

Jäggi A, Dach R, Montenbruck O, Hugentobler U, Bock H, Beutler G (2009) Phase center modeling for LEO GPS receiver antennas and its impact on precise orbit determination. J Geod (accepted for publication, 30 June 2009, online publication 29 July 2009)

Jefferson D, Bar-Sever Y, Heflin M, Watkins M, Webb F, Zumberge J (1999) JPL IGS Analysis Center Report. IGS 1998 Technical Reports, pp 89–97

Kroes R (2006) GRACE: precise relative positioning of formation flying spacecraft using GPS. Dissertation, Delft University, Publications on Geodesy 61 Delft, March 2006, ISBN 10:90-6132-296-0

Laurichesse D, Mercier F, Berthias JP, Broca P, Cerri L (2008) Zero-difference ambiguity fixing for spaceborne GPS receivers. In: Proceedings of ION GNSS 2008, the 21st international technical meeting of the satellite division of the Institute of Navigation, Savannah, Georgia, 16–19 September 2008, pp 758–768

Liu Z, Owen S, Dong D, Lundgren P, Webb F, Hetland E, Simons M (2009) Re-examination of the interplate coupling in Nankai trough, Japan using GPS data in 1996–2006. Geophys J Int (in revision, November)

McCarthy D, Petit G (2004) IERS Conventions (2003) IERS Technical Note No. 32, http://www.iers.org/iers/publications/tn/tn32, Verlag des Bundesamts fur Kartographie und Geodasie, Frankfurt am Main

Melbourne WG (1985) The case for ranging in GPS base systems. In: Proceedings of the first symposium on precise positioning with the global positioning system, positioning with GPS-1985. U.S. Department of Commerce, Rockville, pp 373–386

Neeck SP, Vaze PV (2008) The ocean surface topography mission (OSTM). Proc SPIE 7106

Niell AE (2006) Global mapping functions for the atmosphere delay at radio wavelengths. J Geophys Res 101:3227–3246

Owen SE, Dong D, Webb FH, Newport BJ, Simons M (2006) Deformation of Japan as measured by improved analysis of GEONET data. Eos Trans. AGU, vol 87, issue 52, Fall Meet. Suppl., Abstract G42A-07

Tapley BD, Bettadpur S, Watkins M, Reigber C (2004) The gravity recovery and climate experiment: mission overview and early results. Geophys Res Lett 31(9):L09607. doi:10.1029/2004GL019920

Wubbena G (1985) Software developments for geodetic positions with GPS using TI-4100 code and carrier measurements. In: Proceedings of the first symposium on precise positioning with the global positioning system, positioning with GPS-1985. U.S. Department of Commerce, Rockville, pp 403–412

Zumberge JF, Heflin MB, Jefferson DC, Watkins MM, Webb FH (1997) Precise point positioning for the efficient and robust analysis of GPS data from large networks. J Geophys Res 102(B3):5005–5017